Modelling the transport phenomena and texture changes of chicken breast meat during the roasting in a convective oven

Rabeler, Felix; Feyissa, Aberham Hailu

Published in:
Journal of Food Engineering

Link to article, DOI:
10.1016/j.jfoodeng.2018.05.021

Publication date:
2018

Document Version
Peer reviewed version

Modelling the transport phenomena and texture changes of chicken breast meat during the roasting in a convective oven

Felix Rabeler , Aberham Hailu Feyissa*

Food Production Engineering, National Food Institute, Technical University of Denmark (DTU), Denmark

*Corresponding author:

Søltofts Plads, 2800, Kgs. Lyngby, Denmark

Email address: abhfe@food.dtu.dk, Tel.: +45 45252531

Keywords: COMSOL Multiphysics, heat and mass transfer, poultry meat, quality prediction, thermal processing, transport in porous media

---

Abstract

A numerical 3D model of coupled transport phenomena and texture changes during the roasting of chicken breast meat in a convection oven was developed. The model is based on heat and mass transfer coupled with the kinetics of temperature induced texture changes of chicken breast meat. The partial differential equations of heat and mass transfer as well as the ordinary differential equations that describe the kinetics of the texture changes were solved using COMSOL Multiphysics® 5.2a. The predicted temperature, moisture and texture (hardness, chewiness and gumminess) profiles were validated using experimentally values. The developed model enables the prediction of the texture development inside the chicken meat as function of the process

parameters. The model predictions and measured values show the clear effect of changing process settings on the texture profiles during the roasting process. Overall, the developed model provides deep insights into the local and spatial texture changes of chicken breast meat during the roasting process that cannot be gained by experimentation alone.

1. Introduction

Heat treatment of chicken breast meat is a crucial processing step in households, professional kitchens and large-scale food industries to achieve a safe and high quality product. Roasting of chicken meat in a convection oven is a common process that involves simultaneous heat and mass transfer. However, the roasting affects the microstructure (Feyissa et al., 2013; Wattanachant et al., 2005), texture (Wattanachant et al., 2005) and appearance (Fletcher et al., 2000) of the product and, consequently, its acceptance by the consumer.

The texture of the chicken meat is the highest rated quality attribute for the consumer during consumption (Lawrie and Ledward, 2006) and it is mainly influenced by protein denaturation which leads to fiber shrinkage and straightening (Tornberg, 2005; Wattanachant et al., 2005). Consequently, the microstructure is becoming denser with compact fiber arrangements which results in the toughening of the chicken meat during the heating (Christensen et al., 2000; Lewis and Purslow, 1989; Wattanachant et al., 2005). Moreover, the protein denaturation leads to a reduction of the water holding capacity (WHC) of the chicken breast meat. The unbound water migrates into the spaces between the meat fibers which leads to a toughening of the meat and to the loss of water during the roasting process (Micklander et al., 2002; Tornberg, 2005).

The quality of the final product is mainly controlled by the chef or operator through adjustments of the process settings. However, this is still based on the cook-and-look approach, which relies on the experience and skills of the chef or operator. A number of researchers measured

47 experimentally the texture change of poultry meat with temperature (Barbanti and Pasquini,
48 2005; Wattanachant et al., 2005; Zell et al., 2010) and Rabeler and Feyissa (2017, submitted for
49 publication) developed kinetic models to describe these changes with time. However, to gain the
50 relationship between the process conditions and the texture development inside the chicken meat,
51 the spatial temperature and time history during the roasting process is needed.
52 Mechanistic models of heat and mass transfer (based on fundamental physical laws) are able to
53 predict the temperature and moisture distribution during the cooking process of meat (Feyissa et
54 al., 2013; van der Sman, 2007), beef meat (Kondjoyan et al., 2013; Obuz et al., 2002) or poultry
55 meat (Chang et al., 1998; van der Sman, 2013). However, for the roasting of chicken breast meat
56 only a limited number of mathematical models are available.
57 Chen et al. (1999) developed a model of heat and mass transfer for convection cooking of
58 chicken patties. In their model they described the transport of moisture inside the chicken patties
59 by diffusion, which is a common approach for modelling mass transfer (Huang and Mittal, 1995;
60 Isleroglu and Kaymak-Ertekin, 2016; Kassama et al., 2014). However, the moisture transport
61 during the cooking process cannot be explained adequately by pure diffusion models (Feyissa et
62 al., 2013; van der Sman, 2007). Roasting of chicken breast meat leads to protein denaturation, the
63 shrinkage of the protein network and the reduction of the water holding capacity. This induces a
64 pressure gradient inside the meat and the expulsion of the excess moisture to the surface of the
65 meat.
66 This approach was used by van der Sman (2013) to model the cooking of chicken breast meat in
67 an industrial tunnel oven. The author showed that the model is able to predict the temperature and
68 moisture development inside the chicken meat for cooking temperatures below the boiling point.
69 However, the presented cooking temperatures (45 to 100 °C) and times (up to 160 min) are not

common settings for the roasting of chicken meat in industrial convection ovens, where hot dry air with more than 150 °C is employed (Chen et al., 1999; Guerrero-Legarreta and Hui, 2010). Thussu and Datta (2012) showed that by coupling texture kinetics with physical based models of heat and mass transfer, the texture development during the frying of potato stripes can be predicted. However, for chicken breast meat or other muscle foods no attempt was made to couple kinetic models for textural changes with mechanistic models of heat and mass transfer to predict the local and spatial texture changes.

Therefore, the aim of this study is to first develop a mechanistic model to predict the temperature and moisture profiles of chicken breast meat during the roasting in a convection oven. Our hypothesis is then that by coupling the developed model for heat and mass transfer with the kinetic models of heat induced textural changes for chicken meat, the texture profile during the roasting process can be predicted as function of process parameters. Afterwards, the model predictions will be validated against experimental values.

2. Modelling of transport phenomena and texture changes

2.1. Process description and model formulation

Roasting in a convection oven is a thermal process, where the product is heated at high temperatures (150 - 300 °C) by circulated hot air. The main mechanisms during the roasting of chicken breast meat in a convective oven are illustrated in Fig. 1. Heat is transferred mainly through convection from the surrounding circulated hot air while a conductive heat flux comes from the roasting tray (bottom of chicken breast). The surrounding oven walls are made of polished stainless steel, thus, the effect of radiation is small compared to the convective transport (see section 3.2.1) (Feyissa et al., 2013). The effect of radiation was included in the model by using an estimated effective heat transfer coefficient (combined convective and radiative heat

transfer coefficient, see section 3.2.1) (Kondjoyan and Portanguen, 2008; Sakin-Yilmazer et al., 2012; Zhang and Datta, 2006). The heat is then internally transferred by conduction and convection.

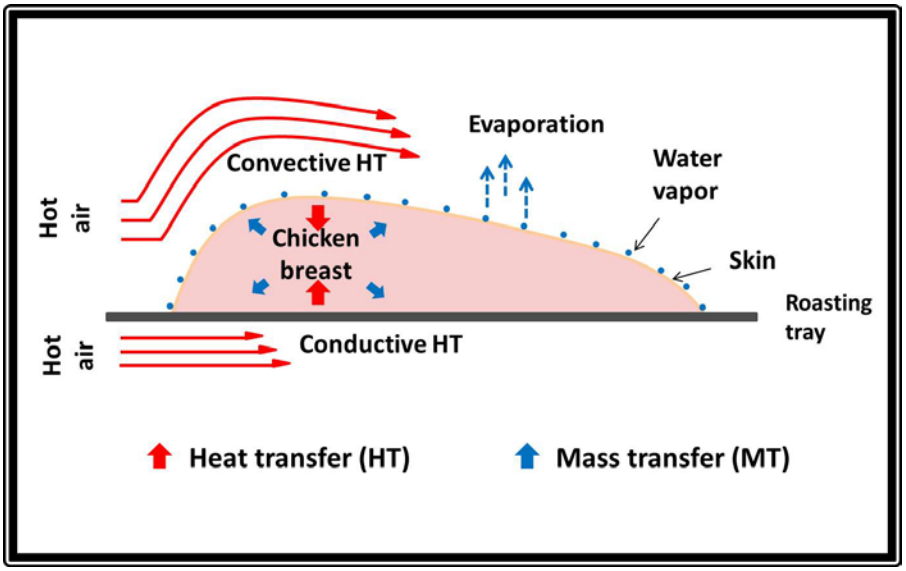

Fig. 1. Schematic illustration of the main mechanisms during the roasting of chicken breast meat in a convection oven.

Water migration within the product takes place by diffusion and convection mechanisms. The latter is a result of the heat induced protein denaturation and shrinkage of the protein network, which results in the decrease of the water holding capacity and a pressure gradient inside the chicken meat. This so called swelling pressure is the driving force for the convective water transport inside the meat and can be described by Darcy's law for flow through porous media (van der Sman, 2007). Liquid water that is expelled to the product surface is then evaporated to the surrounding hot air.

From the measured temperature profiles inside the chicken meat we observed that the temperature stays below the evaporation temperature and only a thin crust is formed during the roasting. Thus, internal evaporation of water was neglected in this study. Furthermore, the following basic assumptions are made to formulate the governing equations for the coupled heat

and mass transfer: fat transport inside the chicken meat is negligible (since the fat content is less than 1% in chicken breast meat), evaporated water consists of pure water (no dissolved matter, measured similar to Feyissa et al. (2013)) and no internal heat generation.

2.2. Governing equations

2.2.1. Heat transfer

The heat transfer within the chicken breast meat is given by Eq. (1) (Bird et al., 2007)

$$c_{p,cm}\,\rho_{cm}\,\frac{\partial T}{\partial t} = \nabla(k_{cm}\,\nabla T) - \rho_w\,c_{p,w}\,u_w\,\nabla T \qquad (1)$$

where $c_{p,cm}$ and $c_{p,w}$ are the specific heat capacities of chicken meat and water (J/(kg K)), respectively, ρ_{cm} and ρ_w are the densities of chicken meat and water (kg/m^3), respectively, k_{cm} is the thermal conductivity of chicken breast meat (W/(m K)), u_w the velocity of the fluid (m/s), T is the temperature (K) and t is the time (s).

2.2.2. Mass transfer

The governing equation for water transport is based on the conservation of mass and is given by Eq. (2) (Bird et al., 2007)

$$\frac{\partial C}{\partial t} = \nabla(-D\,\nabla C + C\,u_w) \qquad (2)$$

where C is the moisture concentration (kg of water/kg of sample) and D is the moisture diffusion coefficient (m^2/s).

Darcy's law gives the relationship between moisture transport and pressure gradient inside a porous medium (in this case meat) and the velocity of the fluid inside the chicken meat can be expressed as

$$u_w = \frac{-\kappa}{\mu_w}\,\nabla p \qquad (3)$$

where κ is the permeability of the chicken meat (m^2), μ_w is the dynamic viscosity of the fluid (Pa s) and ∇p is the pressure gradient vector (Pa/m). The swelling pressure is given by Eq. (4) (Barrière and Leibler, 2003; van der Sman, 2007)

$$p = G'(C - C_{eq}) \quad (4)$$

with *G'* the storage modulus and C_{eq} the water holding capacity of chicken breast meat.

By inserting the expression for the swelling pressure (Eq. (4)) into Eq. (3) the following expression results for the fluid velocity u_w:

$$u_w = \frac{-\kappa\, G'}{\mu_w} \nabla(C - C_{eq}) \quad (5)$$

The storage modulus varies with temperature and was described by with a sigmoidal function (Eq. (6)) (Rabeler and Feyissa, 2017, submitted for publication):

$$G' = G'_{max} + \frac{(G'_0 - G'_{max})}{1+\exp\left(\frac{T-\bar{T}}{\Delta T}\right)} \quad (6)$$

with G'_{max} = 92 kPa (the maximum value of the storage modulus for chicken meat), G'_0 = 13.5 kPa (the initial value of the storage modulus), $\bar{T}$ = 69 °C and ΔT = 4 °C.

The change in the water holding capacity with temperature is described by Eq. (7) (van der Sman, 2013):

$$C_{eq(T)} = y_{w0} - \frac{a_1}{1 + a_2\, exp(-a_3(T - T_\sigma))} \quad (7)$$

where y_{w0} = 0.77 is the initial water content of raw chicken meat, T_σ = 315 K, a_1 = 0.31, a_2 = 30.0 and a_3 = 0.17.

2.3. Initial and boundary conditions

We assume a uniform initial temperature (Eq. (8)) and moisture distribution (Eq. (9)) throughout the whole sample domain (Fig. 2b):

$$T(x, y, z, 0) = T_0 \quad (8)$$

$$C\ (x, y, z, 0) = C_0 \quad (9)$$

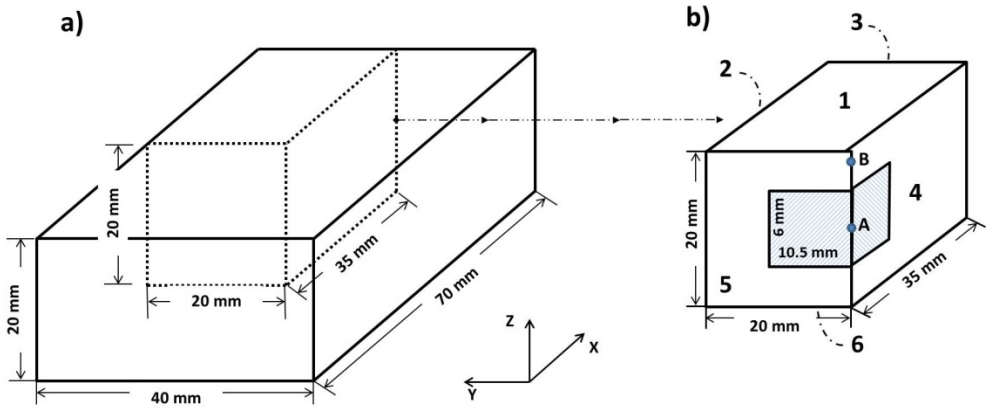

Fig. 2. Schematic illustration of (a) the rectangular chicken meat sample and (b) the geometry used in the developed model. The points: A (0, 0, 10 mm) and B (0, 0, 19mm) indicate the position of the two thermocouples and the striped part shows the domain for the texture validation.

2.3.1. Heat transfer boundary condition

The boundaries 1, 2 and 3 (see Fig. 2) are exposed to the hot air and the heat flux is given by Eq. (10):

$$-k_{cm}\nabla T = h_{eff}\ (T_{oven} - T_{surf}) \quad (10)$$

where k_{cm} is the thermal conductivity of the chicken breast meat (W/(m K)), h_{eff} is the effective heat transfer coefficient (W/(m^2 K)), which is the sum of both the convective and radiative heat transfer (Sakin et al., 2009) (see section 3.2.1) , T_{oven} is the oven temperature (K) and T_{surf} is the surface temperature (K) of the chicken breast meat.

At boundary 6 the chicken meat is in contact with the roasting plate and a heat flux at this boundary is given by Eq. (11):

$$-k_{cm}\nabla T = h_{bot}\ (T_{oven} - T_{bot}) \quad (11)$$

with the heat transfer coefficient h_{bot} and bottom surface temperature T_{bot} (W/(m^2 K)).

Boundaries 5 and 4 are symmetry boundary conditions.

2.3.2. Mass transfer boundary condition

The water evaporation at the boundaries 1, 2, 3 and 6 is given by Eq. (12):

$$-D\,\nabla C + C\,u_w = \beta_{tot}\,(C_{surf} - C_{oven})¤ \qquad (12)$$

where β_{tot} is the mass transfer coefficient (m/s), C_{surf} is the water vapor concentration at the surface of the meat (kg/kg) and C_{oven} the water vapor concentration in the air flow inside the oven.

Van der Sman (2013) reported that the top layer (epimysium connective tissue) of the chicken breast meat becomes glassy during the roasting which results in an increased resistance against water evaporation. To take this into account the author formulated a mass transfer coefficient β_{skin} (Eq. 13)) which is dependent on the local moisture content at the surface of the chicken breast meat.

$$\beta_{skin} = \beta_1\,{y_w}^b \qquad (13)$$

where β_1 and b are 0.040 [m/s] and 4.0 , respectively (van der Sman, 2013).

The total mass transfer coefficient is then given by Eq. (14):

$$\frac{1}{\beta_{tot}} = \frac{1}{\beta_{ext}} + \frac{1}{\beta_{skin}} \qquad (14)$$

where β_{ext} refers to the external mass transfer coefficient which is calculated using the Lewis relation (Eq. (15)):

$$\beta_{ext} = \frac{h}{\rho_a\,c_{p,a}\,Le^{2/3}} \qquad (15)$$

Boundaries 5 and 4 are symmetry boundary conditions.

2.4. Thermo-physical properties

The thermo-physical properties of chicken breast meat were described as function of composition and temperature (including the effect of fiber direction) (Choi and Okos, 1986). For the thermal conductivity we assume that all fibers are oriented along the x-axis (see Fig. 2) of the chicken

breast. The thermal conductivity parallel to the fibers ($k_{cm,\parallel}$) is calculated using the parallel model (Eq. (16)) and for the thermal conductivity perpendicular to the fibers ($k_{cm,\perp}$), we assume the serial model (Eq. (17)).

$$k_{cm,\parallel} = \sum k_i \, \phi_i \quad (16)$$

$$\frac{1}{k_{cm,\perp}} = \sum \frac{\phi_i}{k_i} \quad (17)$$

where k_i and ϕ_i are the thermal conductivities (W/(m K)) and volume fractions of the each component i (water, protein, fat and ash), respectively.

The specific heat capacity (J/(kg K)) of chicken meat is calculated using Eq. (18)

$$c_{p,cm} = \sum y_i \; c_{p,i} \quad (18)$$

where y_i and $c_{p,i}$ are the mass fraction and specific heat capacity of each component i (water, protein, fat and ash), respectively.

2.5. Kinetic model for texture changes

A modified reaction rate law, which is taking into account that foods retain a non-zero equilibrium even after long heating times, was used to describe the texture (hardness, gumminess and chewiness) changes of chicken breast meat with temperature and time (for details see (Rabeler and Feyissa, 2017, submitted for publication)) (Eq. 19):

$$\frac{\partial Q}{\partial t} = k \, (Q_\infty - Q)^n \quad (19)$$

where Q is the quality attribute, Q_∞ is the final non-zero equilibrium quality value after long heating times, k is the reaction rate constant (min^{-1} $[Q]^{1-n}$) and n the reaction order.

The temperature dependence of the reaction rate constant is described by the Arrhenius equation as followed (Eq. (20)):

$$k = k_0 e^{-\frac{E_a}{R\,T}} \quad (20)$$

with k_0 the pre-exponential factor (min^{-1} $[Q]^{1-n}$), E_a the activation energy in J/mol, R is the universal gas constant (8.314 J/(mol K)) and T is the temperature in K.

The modified reaction rate law is coupled with the model for heat and mass transfer (section 2.4), allowing the prediction of the texture parameters hardness, gumminess and chewiness from the local temperature development with time. The estimated activation energies, pre-exponential factors and reaction orders by Rabeler and Feyissa, (2017, submitted for publication) were used to solve Eq. (19) and (20).

2.6. Model solution

The coupled PDEs of heat and mass transfer (equations described in section 2.4) and the kinetic models (ODEs) that describe the quality changes (hardness, gumminess and chewiness) (section 2.5) were implemented and solved using the finite element method (FEM) in the commercial software, COMSOL Multiphysics 5.2a. The model input parameters are shown in Table 1. A rectangular geometry with the dimensions illustrated in Fig. 2b was built in COMSOL and meshed. Mesh sensitivity analysis was conducted, where the mesh size was decreased in a series of simulations until it had no further impact on the model solution (Kumar and Dilber, 2006).

Table 1: Model input parameters

Parameter	Symbol	Value	Unit	Source
Density				
chicken meat	ρ_{cm}	1050	kg/m^3	Calculated from (Choi and Okos, 1986)
water	ρ_w	998	kg/m^3	
Diffusion coefficient	D	3×10^{-10}	m^2/s	(Ngadi et al., 2006)
Permeability	κ	3×10^{-17}	m^2	(Datta, 2006)

Viscosity water	μ_w	0.988 x 10^{-3}	Pa s	
Initial composition				
Water	y_{w0}	0.76	kg/kg	Measured
Protein	y_{p0}	0.22	kg/kg	(Barbanti and Pasquini, 2005)
Fat	y_{f0}	0.01	kg/kg	(Barbanti and Pasquini, 2005)
Ash	y_{a0}	0.01	kg/kg	(Barbanti and Pasquini, 2005)
Latent heat of vaporization of water	H_{evap}	2.3 x 10^6	J/kg	
Initial meat temperature	T_0	6	°C	Measured
Initial moisture concentration	C_0	0.76	kg/kg	Measured
Water vapor concentration in ambient air	C_{air}	0.05	kg/kg	Measured
Heat transfer coefficient				
High fan speed	h_{eff}	44	W/(m^2 K)	Measured
	h_{bot}	59	W/(m^2 K)	
Low fan speed	h_{eff}	21	W/(m^2 K)	Measured
	h_{bot}	41	W/(m^2 K)	

3. Materials and Methods

3.1. Sample preparation and oven settings

Chicken breast meat (skinless and boneless) was purchased from a local supermarket the same day as the experiments and stored in plastic bags at 4 °C until it was used. For all roasting experiments, the chicken breasts were cut into rectangular blocks with the dimensions of 0.04 m x 0.02 m x 0.07 m and a weight of 63 g ± 2 g. The fiber direction for all samples was along the x-axis (see Fig. 2).

A professional convection oven with roasting chamber dimensions of 0.45 m x 0.50 m x 0.65 m was used for the roasting experiments. Dry hot air was circulated inside the roasting chamber by a fan, while the fan speed (air speed) could be adjusted. The oven temperature was controlled by the oven thermostat and additionally two thermocouples were placed at different positions in the oven to measure the oven temperature continuously. The measured oven temperature was stable around the set point with a standard deviation of ± 3 °C. Before each experimental run, the oven was preheated to the desired temperature for 30 min to ensure steady state conditions. The following process settings were used to show the effect of process conditions on the temperature, moisture and texture profile and to validate the developed model:

Setting I: T_{oven} = 170 °C, high fan speed (HF)

Setting II: T_{oven} = 230 °C, high fan speed (HF)

Setting III: T_{oven} = 230 °C, low fan speed (LF)

3.2. Experimental data

3.2.1. Heat transfer coefficient

The combined heat transfer coefficient, which is the sum of the radiative and convective heat transfer coefficient, was estimated using the lumped method (Sakin et al., 2009). The oven was preheated for 30 min before the experiments to ensure steady state conditions. Polished silver and black painted aluminum blocks (rectangular) were placed in the oven and heated for 20 min at 200 °C. The temperature in the center of the blocks was recorded continuously by using a thermocouple. As the Biot number was smaller than 0.1 the lumped heat transfer method was used and the combined heat transfer coefficient estimated as described by Feyissa et al. (2013). Only minor differences (less than 5%) between the estimated heat transfer coefficients for the black and polished aluminum block was found. This means that the radiative heat transfer from

265 the oven walls is small compared to the convective heat transfer. Furthermore, the heat flux by
266 radiation (assuming T_{oven} = 200 °C, $\varepsilon_{chicken}$ = 0.8, T_{surf} = 100 °C) is small (≈ 2 % of the total flux)
267 compared to the convective heat flux. In the model the estimated effective heat transfer
268 coefficient, which includes the radiative effect, was used as described by Kondjoyan and
269 Portanguen (2008), Sakin-Yilmazer et al. (2012) or Zhang and Datta (2006).

270 **3.2.2. Local temperature**

271 In order to measure the temperature profile inside the chicken meat sample, two thermocouples
272 were placed at the center (point A, Fig. 2b)) and close to surface (point B, Fig. 2b) of the sample.
273 One sample was then placed centrally on the roasting tray and the tray positioned in the middle of
274 the oven. The temperature development was measured as function of time with sample intervals
275 of 5 seconds for 15 min (for setting II, see section 3.1) and 20 min (for setting I and III).

276 **3.2.3. Moisture content**

277 To compare the predicted and measured moisture content at different time steps, roasting
278 experiments were performed with different times: 1, 3, 5, 7, 10 and 15 min for all process
279 settings. For setting I and III (see section 3.1), an additional sample was taken at 20 min of
280 roasting. The samples were taken out of the oven after the corresponding roasting time, sealed in
281 plastic bags and placed in ice water to stop further water loss from the surface. The average
282 moisture content of the whole chicken meat sample was then measured using the oven drying
283 method (Bradley, 2010). The samples were minced, weighed in aluminum cups and dried for 24
284 hours at 105 °C. From the weight difference before and after the drying, the moisture content of
285 the chicken meat samples was calculated.

3.2.4. Texture measurements

To validate the predicted texture development, roasting experiments were conducted at different time steps: 3, 5, 7, 10, 15 and 20 min (20 min only for Settings I and III, see section 3.1). After the roasting process, the samples were immediately placed in ice water for 4 min to cool them down quickly. The samples were then stored at room temperature for 2 hours in sealed aluminum cups before the texture measurements.

To measure the textural changes of chicken breast meat, double compression tests (TPA) were performed according to the procedure described by Rabeler and Feyissa (2017, submitted for publication). A cylindrical probe with a height of 6 mm ± 0.5 and a diameter of 21 mm ± 1 was cut out of the middle of the roasted chicken samples using a cork borer. The same sample dimension as in Rabeler and Feyissa (2017, submitted for publication) were used for the TPA measurements. The samples were compressed to a final strain of 40 %, setting the test speed to 1 mm/s with time interval of 5s between the first and second stroke. The TPA parameters hardness, gumminess and chewiness were then calculated from the recorded force-time plot (Bourne, 2002).

3.3. Statistical analysis

The chi-square test was used to evaluate the goodness-of-fit between the model predictions and the experimental data for the temperature, moisture and texture (Eq. 21) (Taylor, 1997):

$$\chi^2 = \sum_{i=1}^{n} \frac{\left(\hat{\theta}_i - \theta_i\right)^2}{{\sigma_i}^2} \qquad (21)$$

with $\hat{\theta}$ the predicted value, θ the measured value and σ the standard deviation. A significance level of $P < 0.05$ was used.

Furthermore, the root mean squared error (RMSE) was calculated by using Eq. (22):

$$RMSE = \sqrt{\frac{\sum_{i=1}^{n}\left(\hat{\theta}_i - \theta_i\right)^2}{n}} \qquad (22)$$

where n is the total number of samples.

4. Results and discussion

4.1. Temperature and moisture predictions

Fig. 3 presents the predicted core (at position A, Fig. 2b) and surface (at position B. Fig. 2b) temperature as well as the predicted average moisture content as function of the roasting time for the different process settings (Fig.3a for setting I, Fig. 3b for setting II, and Fig. 3c for setting III). A good agreement between the measured (symbols) and predicted (solid lines) temperature profiles at the core (*RMSE* = 1.85, 0.83 and 0.99 °C for setting I, II and III, respectively) and close to the surface (*RMSE* = 3.76, 2.69 and 2.6 °C for setting I, II and III, respectively) was found for all tested process settings. Furthermore, the model showed a high accuracy in the prediction of the average moisture content development of the chicken meat sample with *RMSE* values of 1.15, 1.39 and 0.91 % for setting I, II and III, respectively (χ^2 = 4.78, 4.66 and 3.97, respectively, P > 0.05) (see also Fig. 3a to 3c).

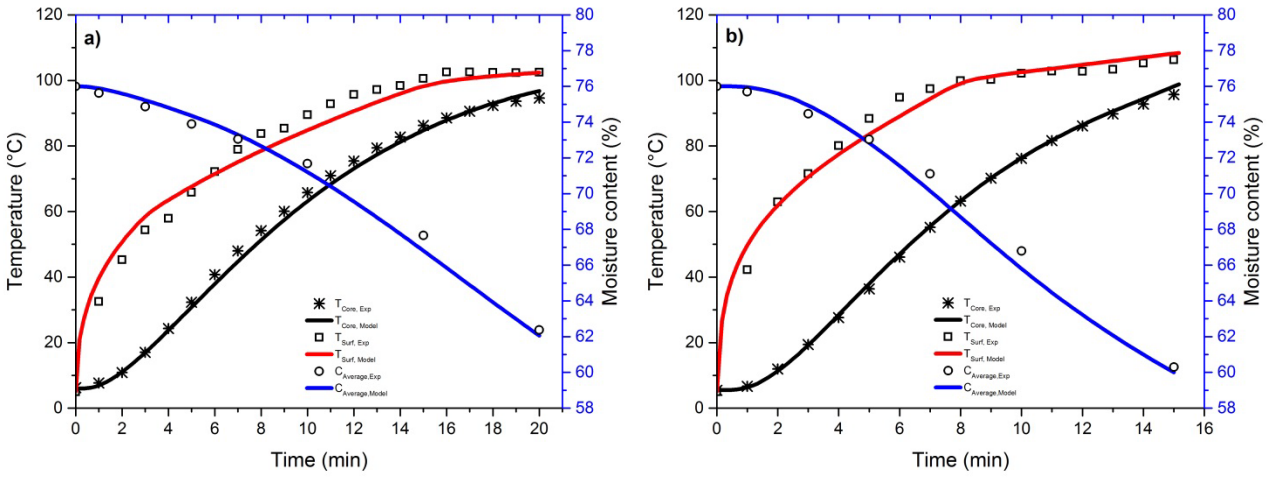

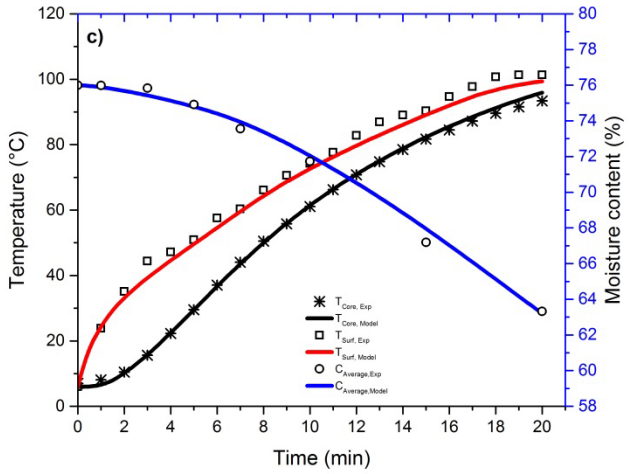

Fig. 3. Comparison between the predicted and measured temperature (core and surface) and moisture development of the chicken meat sample with varying air temperature and fan speed: a) Setting I: Toven = 170 °C, high fan speed; b) Setting II: Toven = 230 °C, high fan speed; c) Setting III: Toven = 230 °C, low fan speed.

323

324 The process conditions have an influence on the temperature and moisture content profile during
325 the roasting process. Chicken breast meat should be heated to a core (coldest point) temperature
326 of 75 °C to ensure a safe product for the consumers (Fsis, 2000). The time needed to reach this
327 temperature in the core varies with the process settings: 12.5 min, 10 min and 13 min roasting
328 time for setting I (T_{oven} = 170 °C and high fan speed, Fig. 3a), setting II (T_{oven} = 230 °C and high
329 fan speed, Fig. 3b) and setting III (T_{oven} = 230 °C and low fan speed, Fig. 3c), respectively.
330 The higher temperature and fan speed for setting II compared to setting I and III, respectively,
331 leads to an increased heat flux from the surrounding hot air to the sample surface. Consequently,
332 the surface temperature is rising faster, which also leads to a faster increase of the core
333 temperature. However, the high surface temperature for setting II results in an increased
334 evaporation of moisture from the chicken meat surface. Therefore, a lower average moisture
335 content is reached for setting II ($C_{av}(t = 10 min) \approx 66$ %, Fig. 3b) compared to setting I ($C_{av}(t$
336 $= 12.5 min) \approx 69$ %, Fig. 3a) and setting III ($C_{av}(t_{75°C} = 13$ min) ≈ 70 %).

Setting I and III show a similar temperature and moisture content development with roasting time (Fig. 3a and 3c, respectively). This is reasonable as the heat flux from the surrounding hot air to the chicken meat surface is comparable for the two settings ($\dot{q}$ = 3080, 5720 and 2730 W/m^2 for setting I, II and III, respectively) (see Eq. 12 and 13). Thus, the times to reach 75 °C in the core as well as the moisture contents at this time step are comparable.

4.2. Prediction of texture changes

By coupling the model for heat and mass transfer with the kinetics for textural changes, it is possible to predict the spatial and local texture change inside the chicken meat from the local temperature development. Fig. 4 presents the simulated temperature and texture distributions inside the chicken meat during the roasting in the convection oven (for setting II, T_{oven} = 230 °C and high fan speed) for 5 min (Fig. 4a and 4c) and 10 min (Fig 4b and Fig. 4d).

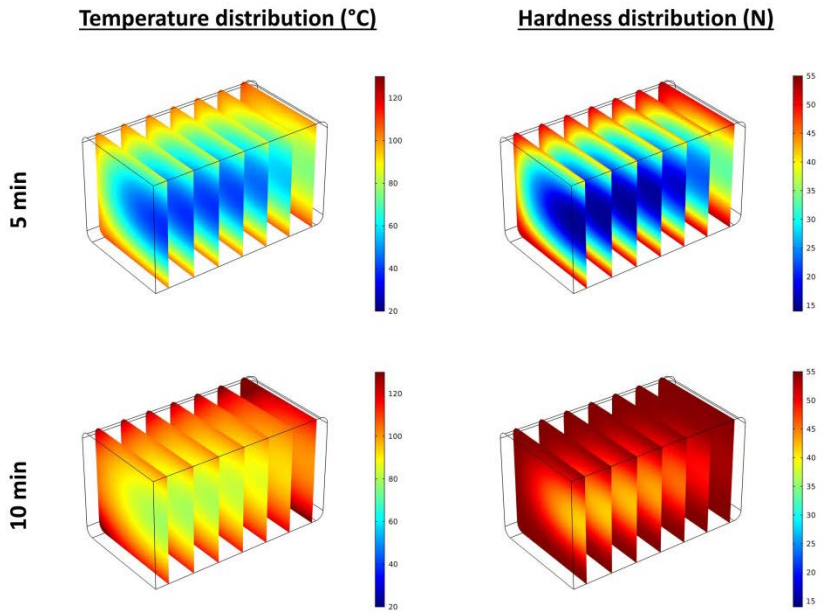

Fig. 4. Visualization of the simulated temperature and hardness distribution during the roasting process: a) temperature profile at t = 5 min; b) temperature profile at t = 10 min; c) hardness profile at t = 5 min; d) hardness profile at t = 10 min. Setting II: Toven = 230 °C, high fan speed.

The results illustrate that the development of the texture parameter hardness, but also the development of the other studied texture parameters (gumminess and chewiness, not shown here), is following the temperature changes. The high heat flux from the surrounding hot air is leading to a fast temperature increase of the chicken meat surface (see also Fig. 3b). This subsequently, results in a fast hardening of the chicken meat at the surface. On the contrary, the internal heat transfer is slow (Bi = 1.1 > 0.1), which leads to a delayed heat up towards the center of the chicken meat. Accordingly, the hardness at the center is changing slower compared to the surface.

Overall, it becomes obvious that the non-uniform temperature development of the chicken meat sample results in the non-uniform texture profiles. The developed model is, therefore, a strong tool to predict the spatial texture development as function of the process conditions and roasting time which is difficult or even not possible to obtain by experimentation alone.

4.3. Effect of process parameters on the texture profile and model validation

In order to study the influence of the oven settings on the texture development of chicken breast meat and to validate the developed model, simulations with two different oven temperatures (230 °C and 170 °C) and fan speeds were compared (see process settings in section 3.1). The predictions of the texture development with roasting time were validated against experimental values that were obtained according to section 3.2.4. Fig. 5a to 5c show that a good agreement between the predicted (solid lines) and experimental measured texture changes (hardness, gumminess and chewiness) (symbols) of chicken breast meat was found for all tested process settings. The *RMSE* and χ^2 values for hardness, gumminess and chewiness are summarized in Table 2. The results further show that the model is able to accurately predict the texture changes of chicken breast meat during roasting for all tested process settings.

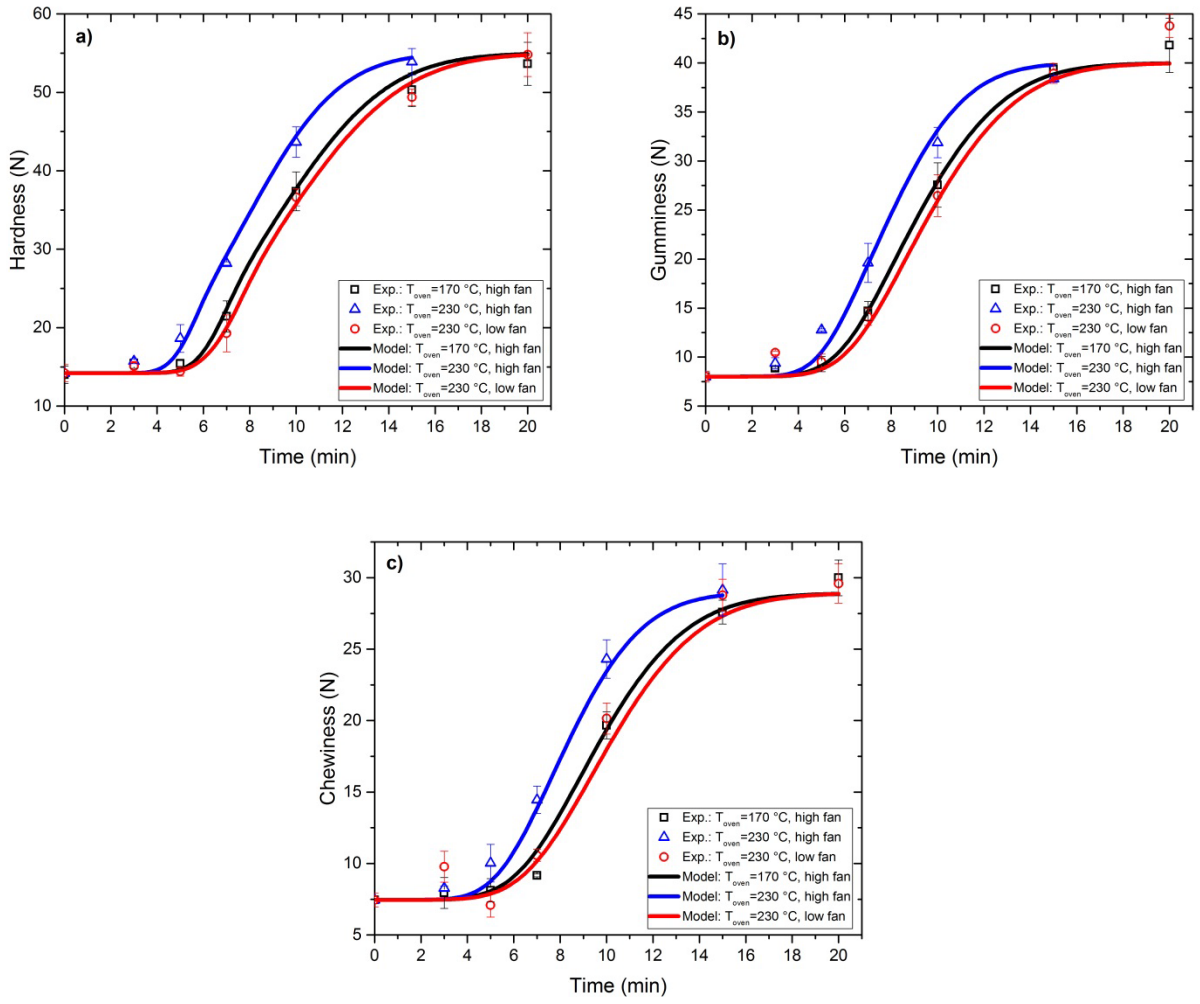

Fig. 5. Effect of process settings on the texture changes of chicken breast meat and comparison between predicted (lines) and experimental values (symbols): a) hardness (N), b) gumminess, c) chewiness. Bars indicate the standard deviation (n = 3).

374

375 **Table 2: RMSE and χ^2 values for hardness, gumminess and chewiness for process setting I, II, and III.**

	Hardness		Gumminess		Chewiness	
	RMSE	χ^2	***RMSE***	χ^2	***RMSE***	χ^2
Setting I	2.06 N	7.12	1.79 N	2.35	2.12 N	7.50
Setting II	1.70 N	2.90	2.11 N	5.12	2.11 N	3.63
Setting III	2.25 N	6.20	2.08 N	6.33	2.73 N	7.17

376

The oven temperature has a high influence on the texture (hardness, gumminess and chewiness) profiles (Fig. 5a to 5c). A higher value of T_{oven} leads to an increased heat flux from the surrounding hot air to the chicken meat surface (see Eq. (10) and Eq. (11)) which results in a faster heat up of the sample (see also Fig. 3a and 3b).Therefore, the texture parameters (that are a function of the local temperature development with time) start to rise earlier for the oven temperature of 230 °C (red line) compared to 170 °C (black line) (setting II and I, respectively). A higher fan speed results in a higher heat transfer coefficient (h_{eff} and h_{bot}, see Table 1) which leads to an increased heat flux to the chicken meat surface (see Eq. (10) and Eq. (11)). Accordingly, the texture parameter rise earlier for the high fan speed (black lines, Fig. 4) compared to the low fan speed (blue lines).

However, only a slight difference in the predicted profiles for hardness, gumminess and chewiness was found between the oven settings I and III (see section 3.1). This is reasonable as a similar temperature development of the two different oven settings was found (compare Fig. 3a with 3c), which results in the similar texture changes.

The predicted changes of the storage modulus with heating time for the tested process settings are presented in Fig. 6. A similar trend between the storage modulus and the TPA parameters hardness, gumminess and chewiness development with time was found for all tested process settings (compare Fig. 6 with Fig. 5a – 5c). Setting II (230 °C, high fan speed) leads to an earlier rise of the storage modulus compared to the lower oven temperature (setting I) and lower fan speed (setting III). Similar to the TPA parameters development only slight differences in the storage modulus development was observed between setting I and III (see Fig. 6). However, we found that the storage modulus starts to rise later (around 55 °C) compared to the texture parameters hardness, gumminess and chewiness (around 45 °C) (compare Fig. 6 with Fig. 5a – 5c). This earlier increase of the TPA parameters could be due to the earlier decrease of the water

holding capacity at around 40 °C which leads to a water release into the pore spaces between the meat fibers (Micklander et al., 2002; van der Sman, 2013). Consequently, parts of the compression energy (TPA measurements) could be dissipated as a result of the viscous flow of the fluid in the pore space which results in a toughening of the meat (Tornberg, 2005) . However, deeper analyses of the heat induced changes in the microstructure of chicken breast meat are necessary to obtain a clear relationship between the storage modulus and the TPA parameters hardness, gumminess and chewiness.

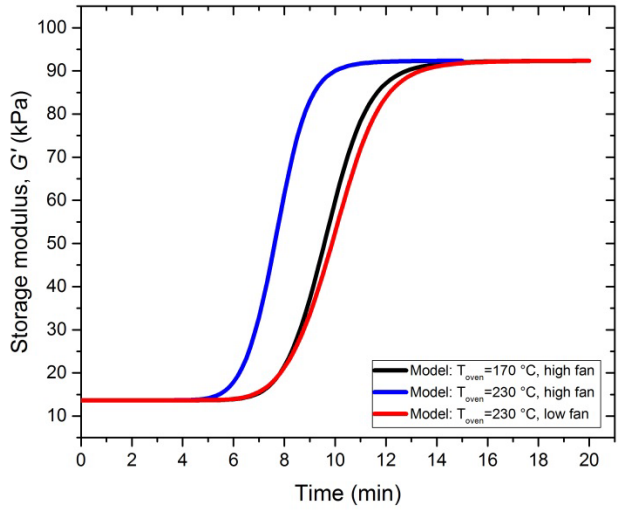

Fig. 6. Predicted storage modulus (G') development with time for the oven settings I (black line), II (blue line) and III (red line).

Overall, the results show that by adjusting the oven settings, the texture of the chicken meat sample can be influenced. Consequently, the developed model can be used to control the quality (texture) of the product and to optimize the roasting process to obtain a safe final product with the highest quality for the consumer.

Conclusion

In this study, a mechanistic model of heat and mass transfer was developed for the roasting of chicken breast meat in a convection oven. The developed model was then coupled with the kinetics for heat induced texture changes. This enabled the prediction of the spatial and local texture development as function of the process parameters. The simulation results were validated against experimental obtained values. The developed model provides a more detailed understanding of the process mechanisms during roasting chicken breast meat.

We showed that the non-uniform temperature distribution inside the chicken meat sample during the roasting process, leads to a non-uniform texture profile. Furthermore, the clear effect of changing roasting parameters on the texture development was obtained. The developed model enables, thus, a deep insight into the effects of the process conditions on the texture changes of chicken breast meat that is difficult or even not possible to obtain by experimentation alone.

Nomenclature

a_w	water activity	Greek symbols	
C	mass concentration (kg/kg)	α	pre-factor (-)
c_p	specific heat capacity (J/(kg K))	β	mass transfer coefficient (m/s)
Cw	chewiness	κ	permeability (m^2)
D	diffusion coefficient (m^2/s)	μ	dynamic viscosity (Pa s)
E_a	activation energy (J/mol)	ρ	density (kg/m^3)
G'	storage modulus (Pa)	ϕ	volume fraction
Gu	Gumminess	$\hat{\theta}_i$	predicted value (T, C, Ha, Gu, Cw)
h	heat transfer coefficient ($W/(m^2 K)$)	θ_i	measured value (T, C, Ha, Gu, Cw)
Ha	hardness (N)	σ	standard deviation
k	reaction rate constant (1/min)	χ^2	chi-square value
k_0	pre-exponential factor (1/min)		
k_i	thermal conductivity (W/(m K))	Subscripts	
M_w	molar weight of water (0.018 kg/mol)		
n	number of samples	a, f, p, w	ash, fat, protein, water
p	swelling pressure (Pa)	bot	bottom
Q	quality attribute	cm	chicken meat
R	universal gas constant (8.314 J/mol K)	eff	effective
T	temperature (K)	eq	equilibrium
t	time (s)	ext	external
u	velocity (m/s)	surf	surface
y	mass fraction	sat	saturation
		tot	total
TPA	texture profile analyses	0	initial (t=0)
Bi	Biot number		
$RMSE$	Root-mean-squared-error		

References

Barbanti, D., Pasquini, M., 2005. Influence of cooking conditions on cooking loss and tenderness of raw and marinated chicken breast meat. LWT - Food Sci. Technol. 38, 895–901. doi:10.1016/j.lwt.2004.08.017

Barrière, B., Leibler, L., 2003. Kinetics of solvent absorption and permeation through a highly swellable elastomeric network. J. Polym. Sci. Part B Polym. Phys. 41, 166–182. doi:10.1002/polb.10341

Bird, R.B., Stewart, W.E., Lightfoot, E.N., 2007. Transport Phenomena, Revised 2n. ed. John Wiley & Sons, Inc.

Bourne, M.C., 2002. Principles of Objective Texture Measurement. Food Texture Viscosity Concept Meas. 2nd Ed.

Bradley, R.L.J., 2010. Food Analysis, in: Nielsen, S.S. (Ed.), Food Analysi S. Springer-Verlag, West Lafayette, IN, USA, pp. 85–104.

Chang, H.C., Carpenter, J.A., Toledo, R.T., 1998. Modeling Heat Transfer During Oven Roasting of Unstuffed Turkeys. J. Food Sci. 63, 257–261. doi:10.1111/j.1365-2621.1998.tb15721.x

Chen, H., Marks, B.P., Murphy, R.Y., 1999. Modeling coupled heat and mass transfer for convection cooking of chicken patties. J. Food Eng. 42, 139–146. doi:10.1016/S0260-8774(99)00111-9

Choi, Y., Okos, M.R., 1986. Effects of temperature and composition on the thermal properties of foods. Food Eng. Process Appl. 93–101.

Christensen, M., Purslow, P.P., Larsen, L.M., 2000. The effect of cooking temperature on mechanical properties of whole meat, single muscle fibres and perimysial connective tissue. Meat Sci. 55, 301–307. doi:10.1016/S0309-1740(99)00157-6

Datta, A.K., 2006. Hydraulic Permeability of Food Tissues. Int. J. Food Prop. 9, 767–780.

doi:10.1080/10942910600596167

Feyissa, A.H., Gernaey, K. V., Adler-Nissen, J., 2013. 3D modelling of coupled mass and heat transfer of a convection-oven roasting process. Meat Sci. 93, 810–820. doi:10.1016/j.meatsci.2012.12.003

Fletcher, D.L., Qiao, M., Smith, D.P., 2000. The relationship of raw broiler breast meat color and pH to cooked meat color and pH. Poult. Sci. 79, 784–788. doi:10.1093/ps/79.5.784

Fsis, U., 2000. Chicken from Farm to Table 1–8.

Guerrero-Legarreta, I., Hui, Y.H., 2010. Handbook of Poultry Science and Technology, Volume 2: ed. John Wiley & Sons, Inc. doi:10.1002/9780470504475

Huang, E., Mittal, G.S., 1995. Meatball cooking - modeling and simulation. J. Food Eng. 24, 87–100. doi:10.1016/0260-8774(94)P1610-A

Isleroglu, H., Kaymak-Ertekin, F., 2016. Modelling of heat and mass transfer during cooking in steam-assisted hybrid oven. J. Food Eng. doi:10.1016/j.jfoodeng.2016.02.027

Kassama, L.S., Ngadi, M.O., Campus, M., 2014. Pore Development and Moisture Transfer in Chicken Meat during Deep-Fat Frying. Dry. Technol. 3937. doi:10.1081/DRT-200054239

Kondjoyan, A., Oillic, S., Portanguen, S., Gros, J.B., 2013. Combined heat transfer and kinetic models to predict cooking loss during heat treatment of beef meat. Meat Sci. 95, 336–344. doi:10.1016/j.meatsci.2013.04.061

Kondjoyan, A., Portanguen, S., 2008. Prediction of surface and “under surface” temperatures on poultry muscles and poultry skins subjected to jets of superheated steam. Food Res. Int. 41, 16–30. doi:10.1016/j.foodres.2007.07.006

Kumar, A., Dilber, I., 2006. Fluid Flow and Its Modeling Using Computational Fluid Dynamics, in: Sablani, S., Datta, A., Shafiur Rehman, M., Mujumdar, A. (Eds.), Handbook of Food and Bioprocess Modeling Techniques, Food Science and Technology. CRC Press.

doi:10.1201/9781420015072

Lawrie, R.A., Ledward, D.A., 2006. Lawrie's meat science.

Lewis, G.J., Purslow, P.P., 1989. The strength and stiffness of perimysial connective tissue isolated from cooked beef muscle. Meat Sci. 26, 255–269. doi:10.1016/0309-1740(89)90011-9

Micklander, E., Peshlov, B., Purslow, P.P., Engelsen, S.B., 2002. NMR-cooking: Monitoring the changes in meat during cooking by low-field 1H-NMR. Trends Food Sci. Technol. 13, 341–346. doi:10.1016/S0924-2244(02)00163-2

Ngadi, M., Dirani, K., Oluka, S., 2006. Mass Transfer Characteristics of Chicken Nuggets. Int. J. Food Eng. 2. doi:10.2202/1556-3758.1071

Obuz, E., Powell, T.H., Dikeman, M.E., 2002. Simulation of Cooking Cylindrical Beef Roasts. LWT - Food Sci. Technol. 35, 637–644. doi:10.1006/fstl.2002.0940

Rabeler, F., Feyissa, A.H., 2017. Kinetic modelling of texture and color changes during thermal treatment of chicken breast meat, (manuscript submitted for publication).

Sakin-Yilmazer, M., Kaymak-Ertekin, F., Ilicali, C., 2012. Modeling of simultaneous heat and mass transfer during convective oven ring cake baking. J. Food Eng. 111, 289–298. doi:10.1016/j.jfoodeng.2012.02.020

Sakin, M., Kaymak-Ertekin, F., Ilicali, C., 2009. Convection and radiation combined surface heat transfer coefficient in baking ovens. J. Food Eng. 94, 344–349. doi:10.1016/j.jfoodeng.2009.03.027

Taylor, J.R., 1997. An introduction to error analysis: the study of uncertainties in physical measurements, 2nd edition. University Science Books.

Thussu, S., Datta, A.K., 2012. Texture prediction during deep frying: A mechanistic approach. J. Food Eng. 108, 111–121. doi:10.1016/j.jfoodeng.2011.07.017

Tornberg, E., 2005. Effects of heat on meat proteins - Implications on structure and quality of meat products. Meat Sci. 70, 493–508. doi:10.1016/j.meatsci.2004.11.021

van der Sman, R.G.M., 2013. Modeling cooking of chicken meat in industrial tunnel ovens with the Flory-Rehner theory. Meat Sci. 95, 940–957. doi:10.1016/j.meatsci.2013.03.027

van der Sman, R.G.M., 2007. Moisture transport during cooking of meat: An analysis based on Flory-Rehner theory. Meat Sci. 76, 730–738. doi:10.1016/j.meatsci.2007.02.014

Wattanachant, S., Benjakul, S., Ledward, D.A., 2005. Effect of heat treatment on changes in texture, structure and properties of Thai indigenous chicken muscle. Food Chem. 93, 337–348. doi:10.1016/j.foodchem.2004.09.032

Zell, M., Lyng, J.G., Cronin, D.A., Morgan, D.J., 2010. Ohmic cooking of whole turkey meat - Effect of rapid ohmic heating on selected product parameters. Food Chem. 120, 724–729. doi:10.1016/j.foodchem.2009.10.069

Zhang, J., Datta, A.K., 2006. Mathematical modeling of bread baking process. J. Food Eng. 75, 78–89. doi:10.1016/j.jfoodeng.2005.03.058